Physically Accurate Fast Nanophotonic Simulations with Physics Informed Model and Training

Ahmet Onur Dasdemir [1], Aykut Erdem [2], and Emir Salih Magden [1,*]

[1] Department of Electrical and Electronics Engineering, Koç University, Sariyer, Istanbul, 34450, Turkey
[2] Department of Computer Engineering, , Koç University, , Sariyer, Istanbul, 34450, Turkey
[*] Corresponding author: esmagden@ku.edu.tr

Abstract

Photonic inverse design has emerged as a powerful technique for creating non-intuitive optical devices, revolutionizing traditional design methodologies. However, the bottleneck in photonic inverse design lies in the computational cost of physically accurate 3D simulations as the high number of optimization iterations or large design foot-print becomes a limiting factor on photonic device design. Here we introduce a novel approach, utilizing a two-staged model combined with a 2D FDFD simulator, to achieve accurate field predictions in a much smaller amount of time than 3D FDTD. The model is trained to emphasize field properties crucial for photonic device optimization such as mode overlap and transmission, enabling rapid and physically accurate simulations. Results demonstrate a remarkable speedup of up to 264.53 times compared to 3D FDTD simulations, opening new avenues for the design of complex and accurate photonic devices.

1 Introduction

1.1 Photonic inverse design

Inverse design has enabled the design of non-intuitive photonic devices that are not possible to design with traditional methods [1, 2, 3, 4]. These traditional methods for designing optical components often rely on manual, iterative processes, which can be time-consuming and limited in their ability to explore the full design space. In contrast, photonic inverse design leverages computational algorithms and machine learning techniques to optimize optical devices with specific desired functionalities. The general design procedure of the photonic inverse design is given in Fig. 1. First, a geometry is initialized with pixel values that correspond to the design variables and electromagnetic simulation of that structure is run to compute the corresponding electric and magnetic fields. Then, performance metrics such as mode overlap and transmission are calculated to find the objective value by comparing the computed performance metrics with the targets. Here, transmission corresponds to the ratio of the output and input power while mode overlap measures the amount of power confined in the desired optical mode. In the final step, an optimization algorithm uses the gradient of the objective function w.r.t the design variables to modify the geometry.

1.2 Simulation bottleneck in inverse design

Finite-difference methods such as Finite-Difference Frequency-Domain (FDFD) and Finite-Difference Time-Domain (FDTD) are most widely used electromagnetic simulation algorithms in photonic inverse design. While 2D versions of these simulation methods are fast, they have a lack of physical accuracy so 3D simulations are used to design devices that shows agreement between

Machine Learning and the Physical Sciences Workshop, NeurIPS 2023.

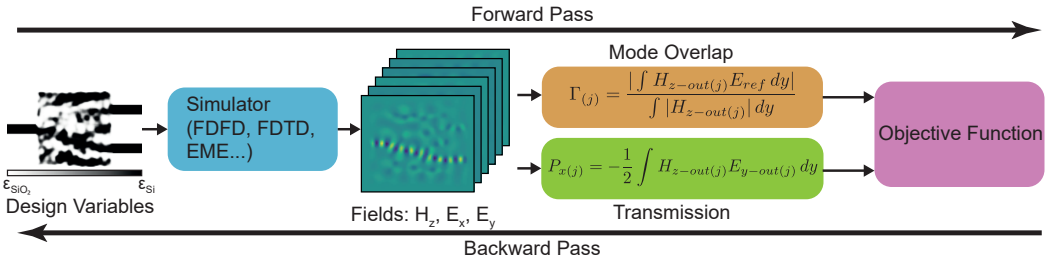

Figure 1: Photonic inverse design scheme. The displayed fields correspond to the TE polarization in 2D simulations, where only nonzero fields are z-component of magnetic field (H_z) and x-y components of electric field (E_x, E_y).

the simulation and experiment measurements. However, due to the high computational cost of 3D simulations, device optimizations that requires many iterations or large foot-prints takes up to many days, limiting the design of photonic devices with complex functionalities [5]. To this end, deep learning approaches replacing the physical simulations have been explored as a promising solution to the aforementioned problem. Previous work includes training a model for predicting 3D FDTD matching fields from the geometry input directly [6], integrating Maxwell's equation to the training for replacing the 2D FDFD [7] and training the simulator and inverse design model at the same time [5]. However, in most previous approaches, models fail to grasp the underlying physics or are limited to 2D physics. As a consequence, they either exhibit a strong dependency on training data or suffer from a lack of physical accuracy. Therefore, a fast and physically accurate deep learning model that is not data dependent and suitable for device optimization is still needed to design complex and non-intuitive devices.

2 Method

2.1 Two staged model

In order to accurately solve the corresponding fields of a device in a short time, we train a two staged model consisting of two u-net layers coupled with a 2D FDFD simulator in between. Flow diagram of our model with the details of the used layers is given in Fig. 2. First, a u-net with residual blocks similar to the one used in [8] modifies the input geometry and then a 2D FDFD simulation is run on the processed geometry. For the TE polarization of light, 2D discretized Maxwell's equations are solved to find the magnetic field H_z and then compute electric fields E_x and E_y from that field. The combination of a learned model and 2D FDFD in this stage has the benefit of preserving the underlying physics of field predictions so that the performance of the model is not data-dependent. However, while the H_z field of a processed geometry may align with physically accurate 3D targets, the computation of E_x and E_y components in the 2D domain may not fully match due to the inherent approximation in 2D simulations. Therefore, although this model is physics informed and helps the generalization, an additional model is necessary to reduce the discrepancy in the computation of E_x and E_y components. For this purpose, a 6-channel intermediate fields, consisting of the real and imaginary parts of the three field components, are fed into a smaller u-net model which refines those fields to match the physically accurate 3D simulations. We note that the prediction of all components, rather than solely H_z, also aids our proposed model in learning the underlying physics.

2.2 Physics informed training

To ensure high generalization performance, we also arrange our training procedure to learn the physics of electromagnetic simulations and the objectives of the photonic device optimization. To this end, we employ the mode overlap and transmission blocks given in Fig. 1 into our loss as shown in Fig. 3. Integration of these physical quantities to our training scheme guides the model to prioritize these field characteristics while also maintaining a good match of fields on the full simulation region. In this way, we prepare our model to excel in generalizing for various photonic device optimization tasks.

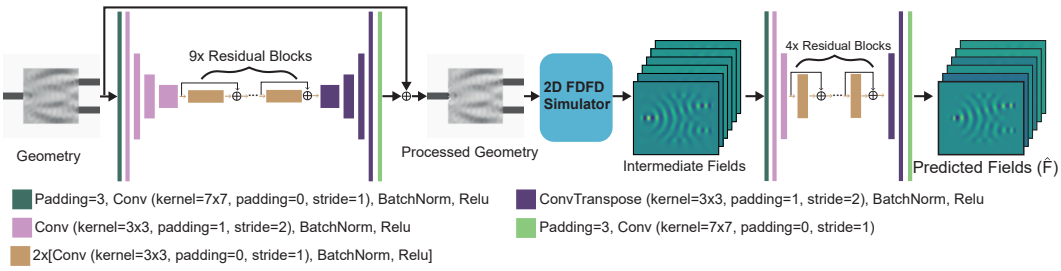

Figure 2: Two staged model scheme

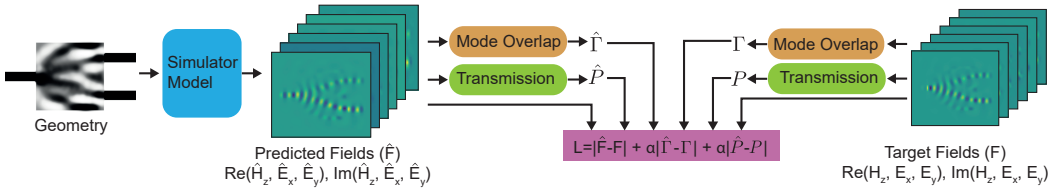

Figure 3: Physics informed training flow diagram

3 Results and Discussion

3.1 Application to test data

We train our model with 6451 samples from our training set and 512 samples are used for validation and test set as well. Further details of our dataset preparation can be found in A.1. To demonstrate the effectiveness of our data on generalizing to unseen samples, we train another model with a u-net that directly processes 2D FDFD fields to match 3D FDTD fields. The corresponding mean absolute error (MAE) results of runs on the test set as well as SSIM measurement to indicate the visual match of fields are provided in Table 1. In addition to the pixel-based losses, physics Notably, our two-staged model, incorporating physics-informed losses, exhibits superior predicted field MAE and SSIM scores. Additionally, mode overlap and transmission results are much closer to the measurements of the target 3D fields. These outcomes signify that our approach relies less on specific data, especially in inverse design tasks involving physical loss quantities, where all data points in the iterations remain unseen.

Table 1: MAE values obtained from standard (U-net on 2D FDFD) model and proposed two staged model.

Model	Field MAE	Mode Overlap MAE	Transmission MAE	Field SSIM
U-net on 2D FDFD	0.0369	0.1287	0.1365	0.8279
Two Staged Model	0.0217	0.0611	0.0137	0.8980

3.2 Application to the design of arbitrary power splitters

To show the performance of two staged model with physically informed losses on the photonic device optimization tasks, we replace it with the simulator block shown in Fig. 1 and perform the inverse design of arbitrary power splitters at $1550\,\mathrm{nm}$ wavelength.These devices divide the light into two ports, each with specified power ratios relative to the input port. After optimizing the devices using our model as a simulator, we run a 3D FDTD simulation on designed geometry to assess physical accuracy of model simulations. The predicted and 3D fields are given in A.2 as well as the geometry of final designed device for one splitting target. The first set of results are given in Table 2 where design region of devices are set to the dimensions used in training set ($4\,\mu\mathrm{m} \times 4\,\mu\mathrm{m}$).Three distinct splitting cases are defined as targets, computed as the product of the desired power ratio and mode overlap, which we aim to equal 1. Termed as "T", we demonstrate that optimizations employing our

Table 2: Inverse design and 3D FDTD results with $4\,\mu\mathrm{m} \times 4\,\mu\mathrm{m}$ device dimensions

Model	Device Size ($\mu\mathrm{m}^2$)	Splitting Target	T (Optimization)	T (3D FDTD)
U-net on 2D FDFD	4×4	0.10-0.90	0.04-0.85	0.02-0.78
Two Staged Model	4×4	0.10-0.90	0.10-0.90	0.06-0.82
U-net on 2D FDFD	4×4	0.30-0.70	0.28-0.67	0.18-0.66
Two Staged Model	4×4	0.30-0.70	0.30-0.70	0.25-0.65
U-net on 2D FDFD	4×4	0.50-0.50	0.49-0.49	0.39-0.47
Two Staged Model	4×4	0.50-0.50	0.50-0.50	0.44-0.45

Table 3: Inverse design and 3D FDTD results with $7\,\mu\mathrm{m} \times 7\,\mu\mathrm{m}$ device dimensions

Model	Device Size ($\mu\mathrm{m}^2$)	Splitting Target	T (Optimization)	T (3D FDTD)
U-net on 2D FDFD	7×7	0.10-0.90	0.00-0.51	0.00-0.40
Two Staged Model	7×7	0.10-0.90	0.08-0.88	0.06-0.79
U-net on 2D FDFD	7×7	0.30-0.70	0.08-0.43	0.03-0.37
Two Staged Model	7×7	0.30-0.70	0.29-0.69	0.23-0.51
U-net on 2D FDFD	7×7	0.50-0.50	0.31-0.27	0.19-0.21
Two Staged Model	7×7	0.50-0.50	0.48-0.49	0.40-0.35

model outperform the standard image processing approach with u-net in reaching the specified target values. More importantly, 3D FDTD results of the designed devices with our suggested approach reaches slightly closer values to the target values. These result indicate that enforcing our model to result in a good mode overlap and transmission values translates to higher physical accuracy in the inverse design of devices.

After demonstrating our model's success on the design of arbitrary splitters with $4\,\mu\mathrm{m} \times 4\,\mu\mathrm{m}$ design region, we extend our application tests to a dimension never before encountered in training, $7\,\mu\mathrm{m} \times 7\,\mu\mathrm{m}$.Table 3 reveals that the standard u-net approach yielded suboptimal results, failing to attain the target values in device optimization. This may be attributed to the potentially limited generalization capability of the standard approach in unfamiliar dimensions, resulting in a less smooth loss landscape and thereby preventing the exploration of desired minima. In contrast, our approach achieved an almost perfect alignment with the optimization targets, and the match with the 3D FDTD measurements was observed reasonable. This indicates that our model has acquired a deep understanding of the underlying physics of electromagnetic simulations, as it performed well in both data and dimensions not included in the training set.

3.3 Simulation run-time speed improvement of our model

After demonstrating exceptional physical accuracy and achieving a successful alignment with 3D FDTD results, we illustrate the significant acceleration in simulation speeds, as shown in Table 4. We measure the time taken to simulate a single device across various dimensions used in our optimization process. With less than one second running time on $4\,\mu\mathrm{m} \times 4\,\mu\mathrm{m}$ devices, our approach showed an impressive 216.66× speedup. With an even greater acceleration for $7\,\mu\mathrm{m} \times 7\,\mu\mathrm{m}$ devices and a strong alignment with optimized results, our two-staged model, trained with physics-informed losses, emerges as a promising approach for the inverse design of photonic devices that would otherwise take days with 3D FDTD simulations.

Table 4: Average run-time comparison for trained model and 3D FDTD simulations

Device Size ($\mu\mathrm{m}^2$)	Model Runtime	3D FDTD Runtime	Speedup Factor
4×4	0.66 s	143 s	216.66×
7×7	1.41 s	373 s	264.53×

4 Conclusion

In summary, we have demonstrated a two staged model trained with physics based losses to achieve highly accurate simulation results in an extremely short amount of time. By combining deep learning techniques with a 2D FDFD simulator and integrating mode overlap and transmission losses into training scheme, we achieved highly accurate simulations at remarkable speeds—up to 264.53 times faster than 3D FDTD. The model's efficacy on matching the 3D FDTD simulation results was validated through diverse testing, showcasing superior performance in device optimization tasks and strong generalization to previously unseen dimensions. These incremental advancements open up possibilities for the design of photonic devices that were previously impractical due to high simulation costs.

Acknowledgments and Disclosure of Funding

This work is supported by Scientific and Technological Research Council of Turkey (TUBITAK) under grant number 122E214.

References

[1] C. M. Lalau-Keraly, S. Bhargava, O. D. Miller, and E. Yablonovitch, "Adjoint shape optimization applied to electromagnetic design," *Optics express*, vol. 21, no. 18, pp. 21693–21701, 2013.

[2] A. Y. Piggott, J. Lu, K. G. Lagoudakis, J. Petykiewicz, T. M. Babinec, and J. Vučković, "Inverse design and demonstration of a compact and broadband on-chip wavelength demultiplexer," *Nature Photonics*, vol. 9, no. 6, pp. 374–377, 2015.

[3] S. Molesky, Z. Lin, A. Y. Piggott, W. Jin, J. Vucković, and A. W. Rodriguez, "Inverse design in nanophotonics," *Nature Photonics*, vol. 12, no. 11, pp. 659–670, 2018.

[4] T. W. Hughes, M. Minkov, I. A. Williamson, and S. Fan, "Adjoint method and inverse design for nonlinear nanophotonic devices," *ACS Photonics*, vol. 5, no. 12, pp. 4781–4787, 2018.

[5] D. Liu, Y. Tan, E. Khoram, and Z. Yu, "Training deep neural networks for the inverse design of nanophotonic structures," *Acs Photonics*, vol. 5, no. 4, pp. 1365–1369, 2018.

[6] M. H. Tahersima, K. Kojima, T. Koike-Akino, D. Jha, B. Wang, C. Lin, and K. Parsons, "Deep neural network inverse design of integrated photonic power splitters," *Scientific reports*, vol. 9, no. 1, p. 1368, 2019.

[7] M. Chen, R. Lupoiu, C. Mao, D.-H. Huang, J. Jiang, P. Lalanne, and J. A. Fan, "High speed simulation and freeform optimization of nanophotonic devices with physics-augmented deep learning," *ACS Photonics*, vol. 9, no. 9, pp. 3110–3123, 2022.

[8] T.-C. Wang, M.-Y. Liu, J.-Y. Zhu, A. Tao, J. Kautz, and B. Catanzaro, "High-resolution image synthesis and semantic manipulation with conditional gans," in *Proceedings of the IEEE conference on computer vision and pattern recognition*, pp. 8798–8807, 2018.

Appendices

Appendix A

A.1 Dataset Preparation

To generate our training data, we create 7475 samples of 140×120 geometry structures which corresponds to $4\,\mu\mathrm{m}\times4\,\mu\mathrm{m}$ design region. 2000 of those samples are generated with random pixels on design region while rest of them are extracted from inverse design optimizations of various devices such as power splitters, filters etc. Some samples from our training set are given in Fig. 4. After creating those geometries to use as input data, 3D FDTD simulations are run and corresponding 2D slices are extracted as target data.

We also note that the geometries has $2\,\mu\mathrm{m}$ additional space around the specified design region including the input-output waveguides and PML.

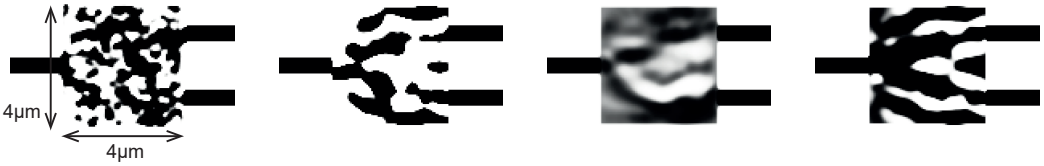

Figure 4: Sample geometries from training set

A.2 Device Optimization Results

Here we demonstrate the designed geometry and field prediction results with comparison to 3D FDTD for the 10/90 splitter designed with $4\,\mu\mathrm{m}\times 4\,\mu\mathrm{m}$ design region. As shown in Fig. 5(a), processed geometry generated after our two stage model's first stage is highly resembling the original geometry. Most of the difference is located around the input waveguide region and design region boundaries, which may be enough to fix the 2D fields to match 3D counterparts. As demonstrated in Fig. 5(b), the field predictions are nearly indistinguishable to the human eye, while also achieving a remarkably low Mean Absolute Error (MAE) and high Structural Similarity Index (SSIM) scores. We also observe that main difference between predictions and targets are located around the output waveguide regions, where we extract the mode overlap and transmission quantities. Given that our model handles these regions differently and aims to align the physical quantities derived from a 1D slice, it is anticipated that while field values around this region may not be an exact match to the targets, the physical quantities do exhibit alignment.

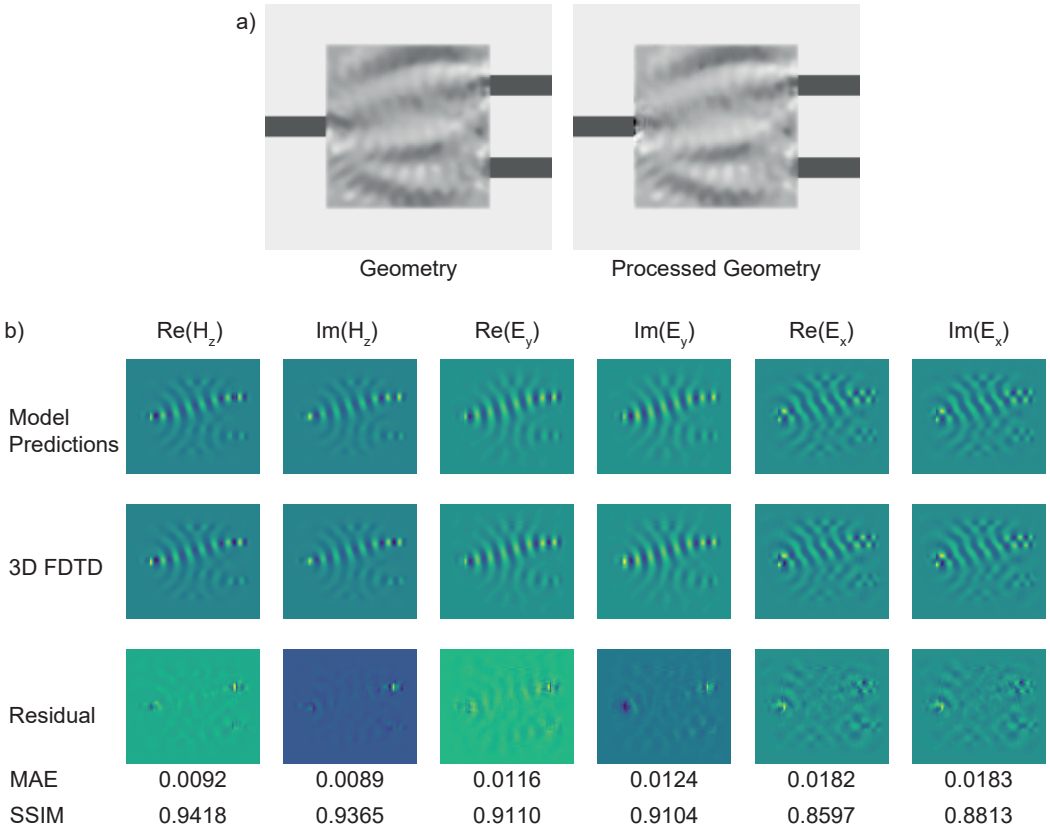

Figure 5: (a) Designed geometry for 10/90 power splitter and corresponding processed geometry generated by model. (b) Model predictions and 3D FDTD results on the final design geometry and residuals showing the difference between them.